Metrol. Meas. Syst., Vol. 25 (2018) No. 2, pp. 331–346.

www.czasopisma.pan.pl www.journals.pan.pl

METROLOGY AND MEASUREMENT SYSTEMS

Index 330930, ISSN 0860-8229

www.metrology.pg.gda.pl

A FAULT VERIFICATION METHOD FOR TESTING OF ANALOGUE ELECTRONIC CIRCUITS

Michał Tadeusiewicz, Stanisław Hałgas

Lodz University of Technology, Faculty of Electrical, Electronic, Computer and Control Engineering, Stefanowskiego 18/22, 90-924 Łódź, Poland (✉ *michal.tadeusiewicz@p.lodz.pl*, +48 42 631 2526, *stanislaw.halgas@p.lodz.pl*)

Abstract

The paper deals with multiple soft fault diagnosis of analogue circuits. A method for diagnosis of linear circuits is developed, belonging to the class of the fault verification techniques. The method employs a measurement test performed in the frequency domain, leading to the nonlinear least squares problem. To solve this problem the Powell minimization method is applied. The diagnostic method is adapted to real circumstances, taking into account deviations of fault-free parameters and measurement uncertainty. Two examples of electronic circuits encountered in practice demonstrate that the method is efficient for diagnosis of middle-sized circuits. Although the method is dedicated to linear circuits it can be adapted to multiple soft fault diagnosis of nonlinear ones. It is illustrated by an example of a CMOS circuit designed in a sub-micrometre technology.

Keywords: analogue circuits, multiple-fault diagnosis, Powell's method, verification technique.

1. Introduction

Fault diagnosis of analogue circuits is of great importance for design validation and has been an active research topic leading to numerous publications, *e.g.* [1–38]. Generally, the diagnosis includes detection of faulty circuits, location of faulty elements and evaluation of their parameters. A fault is said to be soft or parametric if a parameter value is drifted from the tolerance range, but does not lead to some topological changes. If a fault is open or short it is called hard or catastrophic one. Although the fault diagnosis has been of considerable interest for the past decades, there is no all-purpose procedure for diagnosing analogue circuits.

The methods dedicated to the soft fault diagnosis usually employ the simulation-after-test approach, where circuit simulations take place after any diagnosis. They are based on measurements of the voltages at accessible nodes, enabling to create a system of equations with the tested parameters as unknown variables. In real electronic circuits these equations are nonlinear. A wide variety of concepts, methods, and techniques have been developed for soft fault diagnosis of analogue circuits, *e.g.*: the Woodbury formula for matrix theory [27], support vector machine [20, 25], linear programming [28], neural networks [1, 12, 16, 21], fuzzy logic approach [4, 13], wavelet transforms [1, 3], frequency response function [22], V-transform of polynomial coeffi-

Article history: received on Oct. 05, 2017; accepted on Jan. 30, 2018; available online on Jun. 30, 2018, DOI: 10.24425/119558.

cients [26], evolutionary algorithm [16–17], Voltera series [8], statistical methods [23]. Several papers focused on multiple soft fault diagnosis of IC parameters, *e.g.* [30, 32].

In the field of fault diagnosis of analogue circuits the fault verification concept has been commonly used. The fault verification technique is based on the hypothesis that some of the circuit parameters are faulty and the others are either nominal or within their tolerance ranges. Next, this hypothesis is verified taking into account the results of measurements performed during the test phase. The number of the measurement data points can exceed the number of the parameters. For the last decades different fault verification techniques have been applied for soft and hard fault diagnosis in linear and nonlinear analogue circuits, *e.g.* [5, 7, 24, 30, 32]. Numerous works in the diagnosis area are devoted to the case when just one element is faulty, *e.g.* [6, 14, 35, 37–38].

The main result of this paper is a new verification method for the multiple soft fault diagnosis of linear analogue circuits. Unlike many other approaches in this field, the method does not require to know any derivatives and, in consequence, to perform sensitivity analyses of the circuit. It is reliable and easy to implement. During the measurement test, rms values of voltages at some nodes accessible for measurement are determined at different values of frequency. In the post-test stage, minimization without gradients of an error function is performed using the Powell's algorithm [39–40]. The method is efficient for the diagnosis of middle-sized linear circuits. It can be extended to nonlinear circuits including CMOS circuits designed in a sub-micrometre technology.

2. Main idea of presented method

Let us consider a linear AC circuit with n parameters considered as potentially faulty, having one input node accessible for excitation and N output nodes accessible for measurement. To arrange the diagnostic test we apply a function generator to the input and measure the rms values $V^{(l)}(\omega)$, $l = 1, \ldots, N$, of the output voltages at different values of frequency. Let us choose J angular frequencies $\omega_1, \ldots, \omega_J$ and read the rms values of $V^{(l)}(\omega_m)$, $m = 1, \ldots, J$; $l = 1, \ldots, N$, labelled $\widehat{V}_m^{(l)}$. Since each of them depends on frequency ω and parameters $p_1, \ldots, p_n$, we write:

$$\widehat{V}_m^{(l)} = V^{(l)}(\omega_m, \boldsymbol{p}), \qquad m = 1, \ldots, J, \quad l = 1, \ldots, N, \tag{1}$$

where $\boldsymbol{p} = [p_1 \cdots p_n]^{\mathrm{T}}$ and T denotes transposition. To find the parameters $p_1, \ldots, p_n$ fitting the functions $V^{(l)}(\omega_m, \boldsymbol{p})$ to the measured data points $\widehat{V}_m^{(l)}$, for $m = 1, \ldots, J$ and $l = 1, \ldots, N$, we minimize the sum of the squares of errors between $\widehat{V}_m^{(l)}$ and $V^{(l)}(\omega_m, \boldsymbol{p})$:

$$f(\boldsymbol{p}) = \sum_{l=1}^{N} \sum_{m=1}^{J} \left(\widehat{V}_m^{(l)} - V^{(l)}(\omega_m, \boldsymbol{p}) \right)^2 . \tag{2}$$

Several minimization methods can be used to solve this nonlinear least squares problem, including the gradient descent method and the Gauss-Newton method. Unfortunately, the above mentioned methods require partial derivatives (gradients) of the functions $V^{(l)}(\omega_m, \boldsymbol{p})$ with respect to the parameters $p_1, \ldots, p_n$. To find the derivatives the sensitivity analyses of the circuit under test must be carried out at each iteration. This is a time-consuming task. To overcome this drawback a minimization method without gradients should be applied and the Powell's method [39–40] is the one which satisfies this demand. It is an efficient technique that enables solving the nonlinear least squares problem and does not require to know any derivatives. The main idea of the Powell's method is as follows. Starting from an initial guess $\boldsymbol{p}^{(0)}$ the minimum of a function $f(\boldsymbol{p})$ is searched. For this purpose the next iteration $\boldsymbol{p}^{(1)}$ is generated by proceeding successively along each of n base vectors. In any case f is a function of one variable and the minimization can be performed using *e.g.* the Fibonacci method (see the Appendix). This method is fast, efficient and easy to implement. The iteration is then repeated leading to a sequence $\boldsymbol{p}^{(1)}, \boldsymbol{p}^{(2)}, \ldots$. While running this procedure the direction vectors are modified and some improving steps are added. The details are presented in Section 3.

The described approach enables to diagnose circuits in some idealized conditions. It ignores variations of the parameters which are not tested, influence of the self-heating, and measurement uncertainty. To adapt the method to real circumstances we replace the fixed measurement voltages $\widehat{V}_m^{(l)}$, $m = 1, \ldots, J$, $l = 1, \ldots, N$, with some ranges around $\widehat{V}_m^{(l)}$. Next, we create M sets of the voltages, each consisting of JN elements, by random selection from the ranges, assuming a uniform distribution. For each of the sets the Powell method is applied, taking into account the previous results, leading to some ranges of the parameter values. As a result intervals $[p_j^-, p_j^+]$, $j = 1, \ldots, n$ of the parameter values are obtained rather than single values.

A sketch of the proposed algorithm:

1. Choose a number n of the potentially faulty elements which are to be tested, a number N of the measurement nodes and a number J of frequencies, so that JN is much greater than n. Pick convergence tolerances ε, μ, a number of iterations η defined in Section 3, and a number M of sets of the voltage values.
2. Perform the diagnostic test and determine the voltage values $\widehat{V}_m^{(l)}$, $m = 1, \ldots, J$; $l = 1, \ldots, N$.
3. Minimize the error function $f(\boldsymbol{p})$ using the Powell's method, finding the parameter values $p_1, \ldots, p_n$ of the tested elements.
4. Create M sets of the voltage values around $\widehat{V}_m^{(l)}$ and for each of them apply the Powell method considering the result of Step 3. Create the intervals $[p_j^-, p_j^+]$ for $j = 1, \ldots, n$.

3. Minimization procedure using Powell's method

To make the Powell's method [39–40] efficient for the fault diagnosis some modification of a set of the base vectors is introduced.

Let $\boldsymbol{p}^{(0)}$ be an initial guess at the location of the minimum of the function $f(\boldsymbol{p})$, $\boldsymbol{c}_k = [0 \cdots 0\, c_k\, 0 \cdots 0]^{\mathrm{T}}$, where $c_k = 0.1 p_k^{\text{nominal}}$, $k = 1, \ldots, n$, be a set of the base vectors, $\boldsymbol{u}_1, \ldots, \boldsymbol{u}_n$ be direction vectors initially equal to $\boldsymbol{c}_1, \ldots, \boldsymbol{c}_n$, respectively, and $i = 0$. A vector $\boldsymbol{p}^{(0)}$ consists of nominal values of the parameters.

Step 1
Set $\boldsymbol{q}_0 = \boldsymbol{p}^{(i)}$.

Step 2
For $k = 1, \ldots, n$ find the value of λ_k that minimizes $f(\boldsymbol{q}_{k-1} + \lambda_k \boldsymbol{u}_k)$ and set $\boldsymbol{q}_k = \boldsymbol{q}_{k-1} + \lambda_k \boldsymbol{u}_k$.

Step 3
Let $\Delta f_k = f(\boldsymbol{q}_k) - f(\boldsymbol{q}_{k-1})$ for $k = 1, \ldots, n$. Find the subscript r so that $|\Delta f_r| = \max(|\Delta f_k|)$ and $\boldsymbol{u}_r$ is the direction of the maximum decrease over all the direction vectors in Step 2.

Step 4
Set $i := i + 1$.

Step 5
If $f(2\boldsymbol{q}_n - \boldsymbol{q}_0) \geq f(\boldsymbol{q}_0)$ or
$2\left(f(\boldsymbol{q}_0) - 2f(\boldsymbol{q}_n) + f(2\boldsymbol{q}_n - \boldsymbol{q}_0)\right)\left(f(\boldsymbol{q}_0) - f(\boldsymbol{q}_n) - |\Delta f_r|\right)^2 \geq |\Delta f_r|\left(f(\boldsymbol{q}_0) - f(2\boldsymbol{q}_n - \boldsymbol{q}_0)\right)^2$,
then set $\boldsymbol{p}^{(i)} = \boldsymbol{q}_n$ and return to Step 1. Otherwise, proceed to Step 6.

Step 6
Set $\boldsymbol{u}_r = \boldsymbol{q}_n - \boldsymbol{q}_0$.
Step 7
Find λ that minimizes $f(\boldsymbol{q}_0 + \lambda \boldsymbol{u}_r)$ and set $\boldsymbol{p}^{(i)} = \boldsymbol{q}_0 + \lambda \boldsymbol{u}_r$.
Step 8
Repeat Steps 1 through 7.

Stopping criteria are: $\sqrt{\sum_{j=1}^{n}\left(\frac{p_j^{(i)} - p_j^{(i-1)}}{p_j^{(i)}}\right)^2} \leq \varepsilon$ and $\frac{\left|f(\boldsymbol{p}^{(i)}) - f(\boldsymbol{p}^{(i-1)})\right|}{f(\boldsymbol{p}^{(i)}) + f(\boldsymbol{p}^{(i-1)})} \leq \mu$, where ε and μ are convergence tolerances. If the number of iterations exceeds the maximum value β, the process is terminated.

Note: while running the Powell's method numerous functions of one variable are minimized. This task can be efficiently solved using the Fibonacci method whose short description is presented in the Appendix.

4. Numerical examples

To illustrate the method described in Sections 2 and 3 we consider two numerical examples. The diagnosed circuits are shown in Figs. 1 and 2, where nominal values of the parameters are shown. All the operational amplifiers included in the circuits are characterized by a linear model consisting of an input resistor 100 kΩ, an output resistor 100 Ω, and a voltage-controlled current source with a magnification coefficient equal to 1000 A/V. The computations were executed on a PC with an Intel (R) Core (TM) i7-6700 processor. The diagnostic procedure was implemented in the DELPHI programming environment.

Example 1

Let us consider the benchmark Sallen-Key bandpass filter [9] shown in Fig. 1. The circuit was built using a general-purpose operational amplifier LM741 operating in the dual supply mode and was laboratory tested using the measurement system consisting of a digital multimeter and a Tektronix AFG3022 function generator. In the fault-free circuit the actual values of parameters were as follows: $R_1 = 10.06$ kΩ, $R_2 = 19.97$ kΩ, $R_3 = 10.04$ kΩ, $R_4 = 10.03$ kΩ, $R_5 = 10.01$ kΩ, $C_1 = 150.3$ nF, $C_2 = 150.3$ nF. We took into account 15 sets of $n = 3$ parameters: $\{R_1, R_2, R_3\}$, $\{R_1, R_2, C_1\}$, $\{R_1, R_2, C_2\}$, $\{R_1, R_3, C_1\}$, $\{R_2, R_3, C_1\}$, $\{R_3, C_1, C_2\}$,

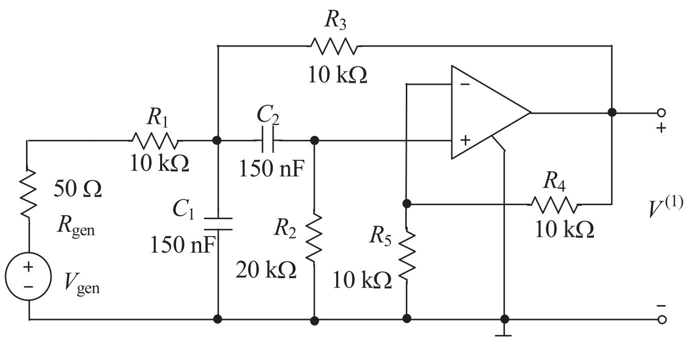

Fig. 1. A Sallen-Key bandpass filter.

$\{R_1, R_2, R_5\}$, $\{R_1, R_3, R_5\}$, $\{R_1, R_4, C_1\}$, $\{R_1, R_5, C_1\}$, $\{R_2, R_3, R_4\}$, $\{R_2, R_3, R_5\}$, $\{R_2, R_4, C_2\}$, $\{R_3, R_4, C_2\}$, $\{R_3, R_5, C_2\}$, which according to the testability analysis [9] could be unambiguously diagnosed. For each of the sets two combinations of the parameter values were assumed. Thus, the total number of diagnoses was 30. We set a fixed rms value of the input voltage ($(V_{\text{gen}})_{rms} = 1$ V) and measured, with an accuracy equal to 10 mV, the rms values of the output voltage $V^{(1)}$ ($N = 1$) at twelve frequencies ($J = 12$) arbitrarily assuming an equal distance between successive frequencies: 50, 59, 68, 77, 86, 95, 105, 114, 123, 132, 141, 150, all in Hz.

To estimate the parameter values the method proposed in this paper was used with the constants: $\varepsilon = 10^{-4}$, $\mu = 0.5 \cdot 10^{-5}$, $\beta = 200$. The ranges around $\widehat{V}_m^{(1)}$ ($m = 1, \ldots, 12$) were chosen assuming the maximum deviation equal to $\pm 1\%$ of the actual value $\widehat{V}_m^{(1)}$. Next, $M = 100$ sets of the voltage values were created by random selection from the ranges assuming a uniform distribution. Every time the minimization procedure was applied it led to the ranges $[p_j^-, p_j^+]$. Having p_j^- and p_j^+ the average value p_j^{av} was calculated and the relative error $\eta_j = \left| \frac{p_j^{\text{actual}} - p_j^{\text{av}}}{p_j^{\text{actual}}} \right| 100\%$ was determined. In all the considered cases the method led to correct results. The results of three representative cases are summarized in Tables 1–3. The average time of the diagnosis process was 1 s.

Table 1. Diagnosis of the set of parameters $\{R_1, R_2, R_3\}$ using the laboratory test.

Parameters p_j	**Nominal value**	**Actual value** p_j^{ac}	**Lower limit** p_j^-	**Upper limit** p_j^+	**Average value** p_j^{av}	**Relative error** η_j [%]
$p_1 = R_1$ [Ω]	10000	7177	6969	7339	7154	0.32
$p_2 = R_2$ [Ω]	20000	22210	22164	22430	22297	0.39
$p_3 = R_3$ [Ω]	10000	8237	8163	8277	8220	0.21

Table 2. Diagnosis of the set of parameters $\{R_2, R_3, C_1\}$ using the laboratory test.

Parameters p_j	**Nominal value**	**Actual value** p_j^{ac}	**Lower limit** p_j^-	**Upper limit** p_j^+	**Average value** p_j^{av}	**Relative error** η_j [%]
$p_1 = R_2$ [Ω]	20000	22210	22051	22367	22209	0.00
$p_2 = R_3$ [Ω]	10000	9082	8876	9134	9005	0.85
$p_3 = C_1$ [nF]	150	115.0	114.3	119.1	116.7	1.48

Table 3. Diagnosis of the set of parameters $\{R_3, C_1, C_2\}$ using the laboratory test.

Parameters p_j	**Nominal value**	**Actual value** p_j^{ac}	**Lower limit** p_j^-	**Upper limit** p_j^+	**Average value** p_j^{av}	**Relative error** η_j [%]
$p_1 = R_3$ [Ω]	10000	8237	8123	8283	8203	0.41
$p_2 = C_1$ [nF]	150	180.0	178.6	183.1	180.9	0.47
$p_3 = C_2$ [nF]	150	180.2	178.7	181.9	180.3	0.06

The parameter deviations considered in the performed 30 diagnoses range from $(-40)\%$ to 76%. The statistical results based on the diagnoses are as follows. In 70% the error η_j does not exceed 1%. The maximum error is 2.7%.

Example 2

In the low pass filter [9] with the parameter values indicated in Fig. 2 we considered ten sets of parameters $\{R_8, R_{17}, C_1, C_3, C_4\}$, $\{R_8, C_1, C_2, C_3, C_4\}$, $\{R_4, R_8, R_{17}, C_3, C_4\}$, $\{R_4, R_8, R_9, R_{17}, R_{21}\}$, $\{R_4, R_8, R_{17}, R_{22}, C_1\}$, $\{R_4, R_8, R_{17}, C_1, C_3\}$, $\{R_4, R_7, R_8, R_{17}, R_{22}\}$, $\{R_4, R_8, C_2, C_3, C_4\}$, $\{R_4, R_6, R_8, R_{17}, R_{19}\}$, and $\{R_4, R_6, R_8, R_{17}, C_4\}$ as potentially faulty. According to the testability analysis [9], they could be unambiguously diagnosed. To perform the diagnosis the method presented in this paper was applied using the tests simulated numerically. We set a fixed rms value of the input voltage ($(V_{\text{gen}})_{rms} = 2$ V) and measured the rms values of the output voltage $V_m^{(1)}$ ($N = 1$), with an accuracy equal to 100 µV, at twenty frequencies ($J = 20$) located at the same distance on a linear scale, with the lower frequency equal to 300 Hz and the upper one equal to 2 kHz. To estimate the parameter values we used the method proposed in this paper with the constants: $\varepsilon = 10^{-4}$, $\mu = 0.5 \cdot 10^{-6}$, $\beta = 500$. The ranges around $\widehat{V}_m^{(1)}$ ($m = 1, \ldots, 20$) were chosen assuming the maximum deviation equal to $\pm 0.5\%$ of the actual value $\widehat{V}_m^{(1)}$. Next $M = 60$ sets of the voltage values were created by random selection from the ranges assuming a uniform distribution leading to the ranges $[p_j^-, p_j^+]$, the average values p_j^{av}, and the relative errors η_j. In all the considered cases the method led to correct results, but in two

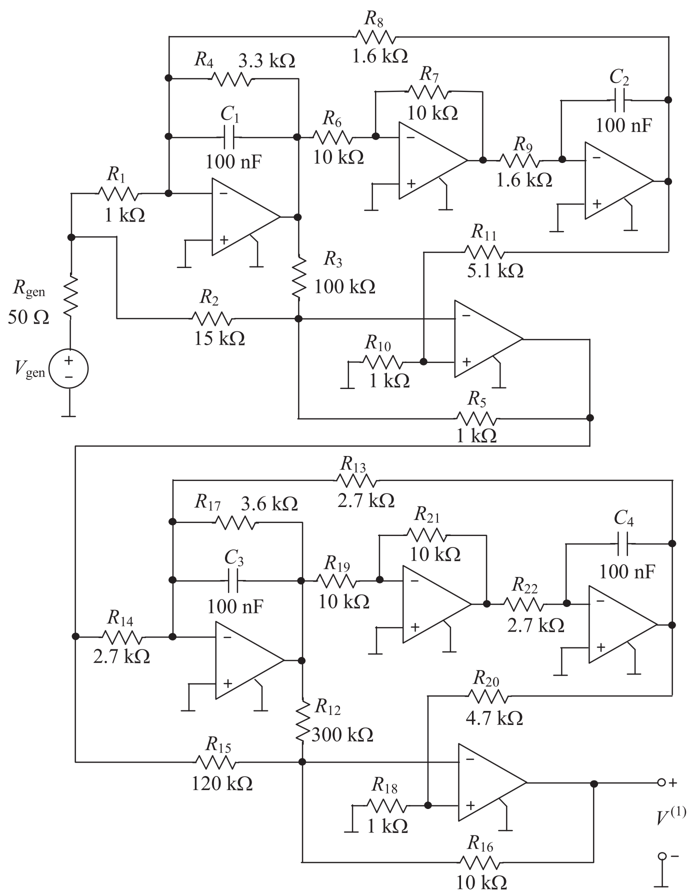

Fig. 2. A low-pass filter.

cases (one of them is shown in Table 6) the obtained intervals for some parameters were rather wide, due to small sensitivity of the output voltage to changes of some parameters. The results of three exemplary cases are summarized in Tables 4–6. The average time of the diagnosis process was 50 s.

Table 4. Diagnosis of the set of parameters $\{R_8, C_1, C_2, C_3, C_4\}$ using the numerical test.

Parameters p_j	**Nominal value**	**Actual value** p_j^{ac}	**Lower limit** p_j^-	**Upper limit** p_j^+	**Average value** p_j^{av}	**Relative error** η_j [%]
$p_1 = R_8$ [Ω]	1600	2600	2579	2642	2610	0.40
$p_2 = C_1$ [nF]	100.0	92.0	88.64	94.44	91.5	0.50
$p_3 = C_2$ [nF]	100.0	150.0	144.60	157.10	150.8	0.57
$p_4 = C_3$ [nF]	100.0	120.0	116.42	123.50	119.9	0.03
$p_5 = C_4$ [nF]	100.0	120.0	115.54	123.76	119.6	0.29

Table 5. Diagnosis of the set of parameters $\{R_4, R_8, R_9, R_{17}, R_{21}\}$ using the numerical test.

Parameters p_j	**Nominal value**	**Actual value** p_j^{ac}	**Lower limit** p_j^-	**Upper limit** p_j^+	**Average value** p_j^{av}	**Relative error** η_j [%]
$p_1 = R_4$ [Ω]	3300	2480	2350	2593	2471	0.34
$p_2 = R_8$ [Ω]	1600	1890	1873	1907	1890	0.00
$p_3 = R_9$ [Ω]	1600	1200	1180	1216	1198	0.17
$p_4 = R_{17}$ [Ω]	3600	2780	2736	2817	2776	0.13
$p_5 = R_{21}$ [Ω]	10000	12000	11845	12201	12023	0.19

Table 6. Diagnosis of the set of parameters $\{R_8, R_{17}, C_1, C_3, C_4\}$ using the numerical test.

Parameters p_j	**Nominal value**	**Actual value** p_j^{ac}	**Lower limit** p_j^-	**Upper limit** p_j^+	**Average value** p_j^{av}	**Relative error** η_j [%]
$p_1 = R_8$ [Ω]	1600	2200	2137	2229	2183	0.77
$p_2 = R_{17}$ [Ω]	3600	2300	2100	2575	2337	1.63
$p_3 = C_1$ [nF]	100.0	150.0	148.08	151.45	149.8	0.16
$p_4 = C_3$ [nF]	100.0	120.0	100.71	134.99	117.8	1.79
$p_5 = C_4$ [nF]	100.0	80.0	72.42	91.86	82.1	2.67

The absolute values of parameter deviations, considered in the performed 10 diagnoses, range from $(-36)\%$ to 60%. The statistical results based on the performed diagnoses are as follows. In 80% the error η_j does not exceed 1%. The maximum error is 3.55%.

The assumed deviations of the output voltages in the chosen circuits correspond to low tolerances of the circuit components. It is justified because the active filters shown in Figs. 1 and 2 can achieve good accuracy, provided that low-tolerance resistors and capacitors are used. Monte Carlo analyses of the circuit depicted in Fig. 1 show that ±1% tolerances cause the output voltage deviations of up to ±4%. Assuming such deviations the obtained diagnostic results are less accurate but quite satisfactory. *E.g.*, for the cases presented in Tables 1, 2, 3 the results obtained with the method with ±4% deviations of the output voltage are summarized in Tables A1, A2, A3, respectively. Also, in Example 2, an increase of the voltage deviations from ±0.5% to ±1.5% leads to quite good results illustrated in Table A4 corresponding to Table 4.

Table A1. Diagnosis of the set of parameters $\{R_1, R_2, R_3\}$ using the laboratory test.

Parameters p_j	**Nominal value**	**Actual value** p_j^{ac}	**Lower limit** p_j^-	**Upper limit** p_j^+	**Average value** p_j^{av}	**Relative error** η_j [%]
$p_1 = R_1$ [Ω]	10000	7177	6311	7857	7084	1.30
$p_2 = R_2$ [Ω]	20000	22210	21851	22748	22299	0.40
$p_3 = R_3$ [Ω]	10000	8237	8001	8400	8200	0.44

Table A2. Diagnosis of the set of parameters $\{R_2, R_3, C_1\}$ using the laboratory test.

Parameters p_j	**Nominal value**	**Actual value** p_j^{ac}	**Lower limit** p_j^-	**Upper limit** p_j^+	**Average value** p_j^{av}	**Relative error** η_j [%]
$p_1 = R_2$ [Ω]	20000	22210	21603	22367	21985	1.01
$p_2 = R_3$ [Ω]	10000	9082	8469	9437	8948	1.47
$p_3 = C_1$ [nF]	150	115.0	102.8	129.0	115.9	0.78

Table A3. Diagnosis of the set of parameters $\{R_3, C_1, C_2\}$ using the laboratory test.

Parameters p_j	**Nominal value**	**Actual value** p_j^{ac}	**Lower limit** p_j^-	**Upper limit** p_j^+	**Average value** p_j^{av}	**Relative error** η_j [%]
$p_1 = R_3$ [Ω]	10000	8237	7781	8502	8141	1.16
$p_2 = C_1$ [nF]	150	180.0	173.3	192.5	182.9	1.61
$p_3 = C_2$ [nF]	150	180.2	174.9	184.1	179.5	0.39

Table A4. Diagnosis of the set of parameters $\{R_8, C_1, C_2, C_3, C_4\}$ using the numerical test.

Parameters p_j	**Nominal value**	**Actual value** p_j^{ac}	**Lower limit** p_j^-	**Upper limit** p_j^+	**Average value** p_j^{av}	**Relative error** η_j [%]
$p_1 = R_8$ [Ω]	1600	2600	2513	2678	2595	0.17
$p_2 = C_1$ [nF]	100.0	92.0	77.75	106.02	91.9	0.12
$p_3 = C_2$ [nF]	100.0	150.0	136.71	171.26	154.0	2.66
$p_4 = C_3$ [nF]	100.0	120.0	108.70	127.55	118.1	1.56
$p_5 = C_4$ [nF]	100.0	120.0	110.11	133.10	121.6	1.34

5. Comparison of results

The methods for fault diagnosis of analogue circuits are based on measurement tests performed in the DC, AC or transient states. Most of them exploit DC or AC state. Numerous results in the parametric diagnosis area relate to circuits with single, double or triple faults with the parameter deviations not exceeding 30% of the nominal values. For example, the references [6, 14, 35, 37–38] are dedicated to soft fault diagnosis of single faults. The references [18, 28–29, 34] bring methods for single-, double-, and triple-fault diagnosis. For this purpose the simplex method is used in [28] and the Woodbury formula in the matrix theory is applied in [29]. A drawback of these methods is the required access to many nodes during the test phase. In the reference [34] the Fisher information measure is exploited, whereas the reference [18] presents an approach based on the intelligent information processing technology.

The multiple-fault diagnosis, not limited only to double or triple faults and small parameter deviations, is more complex and insufficiently resolved. Some results of the general multiple soft fault diagnosis are presented in the references [15] and [36]. They employ a measurement test performed in the DC or AC state and some computational techniques. Unfortunately, the approach proposed in [36] requires higher-order sensitivity analyses what is a very time-consuming task. In consequence, the application of this method is limited to small-sized circuits. The method proposed in [15] relates to larger and more complex circuits and is compared below, head to head, with the method presented in this paper. For the sake of comparison the method presented in this paper is labelled MA, whereas the method used in the reference [15] is labelled MB.

In order to compare MA and MB we reconsider the low pass filter shown in Fig. 2 and take into account elements of the set $\{C_1, C_2, C_3, C_4, R_4, R_8, R_{17}, R_{21}\}$ as possibly faulty. Let us create eleven sets of the parameters: $\{R_8, C_1, C_2, C_3, C_4\}$, $\{R_8, R_{17}, C_1, C_3, C_4\}$, $\{R_4, R_8, R_{17}, C_3, C_4\}$, $\{R_8, R_{21}, C_3, C_4\}$, $\{R_4, R_{17}, C_3, C_4\}$, $\{R_4, R_8, R_{17}, R_{21}\}$, $\{R_8, C_1, C_2, C_4\}$, $\{C_1, C_2, C_3\}$, $\{R_4, R_8, R_{17}\}$, $\{R_4, R_{21}, C_1\}$, and $\{R_4, R_8, C_3\}$. To arrange the diagnostic test we set a fixed rms value of the input voltage ($(V_{\text{gen}})_{rms} = 2$V) and find the output voltage $V_m^{(1)}$ ($N = 1$), with an accuracy equal to 100 μV at twenty frequencies ($J = 20$), as in Example 2. The constants used by MA are: $\varepsilon = 10^{-4}$, $\mu = 0.5 \cdot 10^{-6}$, $\beta = 500$. The comparison has been performed under the following assumptions.

(i) The sets of parameters are diagnosed assuming nominal values of other parameters and fixed measurement data. In consequence, the methods give points rather than ranges of the parameter values.

(ii) Since the MA method requires rms values of the measured voltages and the MB method requires phasor values, the number of data points exploited by MB is twice as large as the number of points exploited by MA. Hence, the number of diagnostic equations used by MA is 20 while by MB is 40.

(iii) The parameter variations selected for the purpose of comparison range from 2.8% to 65% of their nominal values.

On the basis of eleven carried out diagnoses the following conclusions can be drawn. The MA method leads to correct results in all the cases, whereas the MB method fails in three cases. MA works with a smaller number of diagnostic equations than MB and it does not require the time-consuming sensitivity analyses. In consequence, the MA method is easier to implement and involves simpler computational analysis. Usually, the parameter values provided by MA are more accurate than those of MB. The results of four chosen diagnoses carried out using MA and MB methods are summarized in Tables 7–10.

Table 7. Diagnosis of the set of parameters $\{R_8, C_1, C_2, C_3, C_4\}$ using the numerical test.

Parameters p_j	**Nominal values**	**Actual values** p_j^{ac} **(Deviation in %)**	**Method A**	**Method B**
$p_1 = R_8$ [Ω]	1600	2600 (62.5%)	2600	Fail
$p_2 = C_1$ [nF]	100.0	92.0 (−8.0%)	92.06	
$p_3 = C_2$ [nF]	100.0	150.0 (50.0%)	149.94	
$p_4 = C_3$ [nF]	100.0	120.0 (20.0%)	120.02	
$p_5 = C_4$ [nF]	100.0	120.0 (20.0%)	120.01	

Table 8. Diagnosis of the set of parameters $\{R_4,\ R_8,\ R_{17},\ C_3,\ C_4\}$ using the numerical test.

Parameters p_j	**Nominal values**	**Actual values** p_j^{ac} **(Deviation in %)**	**Method A**	**Method B**
$p_1 = R_4$ [Ω]	3300	3420 (3.6%)	3427	3409
$p_2 = R_8$ [Ω]	1600	1420 (−11.3%)	1420	1420
$p_3 = R_{17}$ [Ω]	3600	3850 (6.9%)	3855	3855
$p_4 = C_3$ [nF]	100.0	120.0 (20.0%)	119.85	120.50
$p_5 = C_4$ [nF]	100.0	82.00 (−18.0%)	82.12	82.98

Table 9. Diagnosis of the set of parameters $\{R_8,\ R_{21},\ C_1,\ C_2\}$ using the numerical test.

Parameters p_j	**Nominal values**	**Actual values** p_j^{ac} **(Deviation in %)**	**Method A**	**Method B**
$p_1 = R_8$ [Ω]	1600	2040 (27.5%)	2040	Fail
$p_2 = R_{21}$ [Ω]	10000	8200 (−18.0%)	8199	
$p_3 = C_1$ [nF]	100.0	150.0 (50.0%)	150.03	
$p_4 = C_2$ [nF]	100.0	103.0 (3.0%)	102.95	

Table 10. Diagnosis of the set of parameters $\{R_8,\ R_{21},\ C_1,\ C_2\}$ using the numerical test.

Parameters p_j	**Nominal values**	**Actual values** p_j^{ac} **(Deviation in %)**	**Method A**	**Method B**
$p_1 = R_8$ [Ω]	1600	2040 (27.5%)	2040	2040
$p_2 = R_{21}$ [Ω]	10000	9800 (−2.0%)	9801	10230
$p_3 = C_1$ [nF]	100.0	115.0 (15.0%)	114.94	114.88
$p_4 = C_2$ [nF]	100.0	103.0 (3.0%)	103.04	103.28

6. Possibility of extension of presented method to nonlinear circuits

Although the method presented in Sections 2 and 3 is dedicated to linear circuits, it can be applied to the multiple soft fault diagnosis of nonlinear ones, including CMOS circuits designed in a sub-micrometre technology. This section explains how the diagnostic method is extended to nonlinear CMOS circuits with soft faults being variations of channel lengths L. The proposed diagnostic method estimates values of the parameters (channel lengths L) belonging to predefined sets of parameters. Comparing them with the nominal or drawn values we can select the ones which can be considered as faulty. Let us consider a circuit having one or more input nodes accessible for excitation and one output node accessible for measurement. To apply the diagnostic method leading to n parameter values $p_1, \ldots, p_n$ we connect $J > n$ sets of DC voltage sources to the input nodes and measure the corresponding DC values of the output voltage $\widehat{V}_1, \ldots, \widehat{V}_J$. Each of the voltage values depends on the parameter values $p_1, \ldots, p_n$, $V_m(\boldsymbol{p})$, where $\boldsymbol{p} = [p_1 \cdots p_n]^{\mathrm{T}}$, $m = 1, \ldots, J$. Hence, in order to find $p_1, \ldots, p_n$, the function:

$$g(\boldsymbol{p}) = \sum_{m=1}^{J} \left(\widehat{V}_m - V_m(\boldsymbol{p})\right)^2 \tag{3}$$

is minimized using the Powell method, as described in Section 3. Since functions $V_m(\boldsymbol{p})$ cannot be presented in the explicit analytical form, their values are found numerically, by the DC circuit analysis, for given values of the parameters.

For the fault diagnosis of CMOS circuits designed in a sub-micrometre technology the proposed method has been implemented in the DELPHI, whereas the required analyses of the circuits for different sets of parameter values are carried out applying the IsSPICE 4 program [41]. Both environments have been joined. The analyses are very complex, because the MOS model BSIM 4.6 is very complicated and described by several hundred equations. In consequence, the total CPU time consumed by the procedure is long. Most of the time is spent on communication between both environments, including the process of creating new input files and deleting old input files for IsSPICE, searching output files, opening and closing the windows.

Example 3

Consider the rail-to-rail input buffer [42] shown in Fig. 3 designed in a nanometre technology. The transistors are characterized by the BSIM 4.6 model implemented in IsSPICE 4, Level 14 [41].

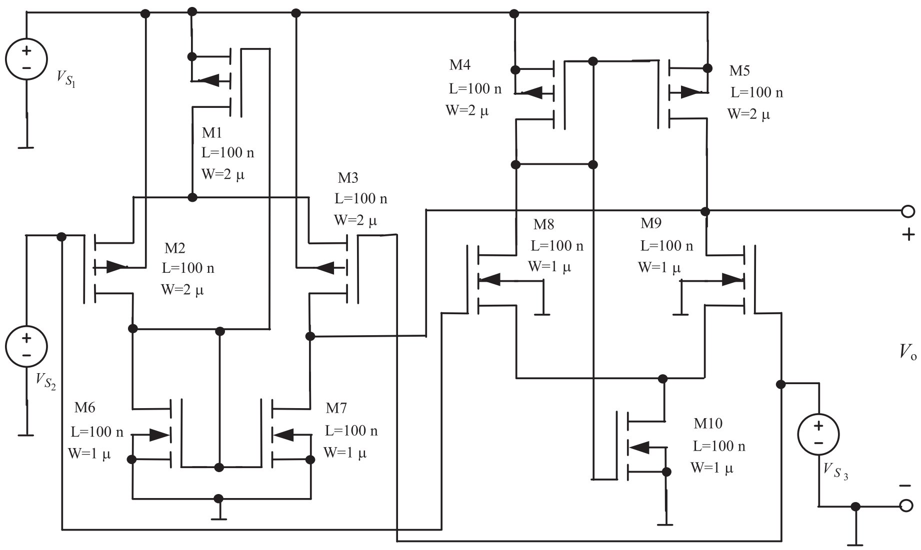

Fig. 3. A rail-to-rail input buffer.

We consider the soft faults of the following parameters:

(i) The channel lengths in PMOS transistors M1, M2, M3, M4, M5.

(ii) The channel lengths in NMOS transistors M6, M7, M8, M9, M10.

The diagnostic test in this example is simulated numerically. For this purpose ten sets ($J = 10$) of the input DC voltages V_{S_1}, V_{S_2} and V_{S_3}, presented in Table 11, are chosen and every time the output voltage V_o is found with an accuracy of 10 μV. To illustrate the method, six sets of faults were diagnosed. The results of two representative cases are summarized in Tables 12–13.

Note: the component deviations considered in this example do not exceed 20%. However, the method works even if the deviations are much greater. Several other cases were diagnosed with the deviations of the order of (30–65)% and the obtained results are quite satisfactory. One of them is summarized in Table 14.

Table 11. Example 3 – Sets of input voltages exploited in the DC diagnostic tests.

No	Values of the input voltages in volts		
	V_{S_1}	V_{S_2}	V_{S_3}
1	1.00	0.50	0.35
2	1.00	0.50	0.40
3	1.00	0.50	0.42
4	1.00	0.65	0.35
5	1.00	0.65	0.40
6	1.30	0.65	0.42
7	1.30	0.65	0.46
8	1.30	0.80	0.60
9	1.30	0.80	0.70
10	1.30	0.80	0.72

Table 12. Example 3 – Results of the fault diagnosis of channel lengths in PMOS transistors M1, M2, M3, M4, M5 (computational time 615 s).

Symbols of the PMOS transistors	M1	M2	M3	M4	M5
The nominal value of L in nm	100.000	100.000	100.000	100.000	100.000
The actual value of L in nm	120.000	108.000	120.000	108.000	107.000
The values provided by the method in nm	119.775	108.007	119.955	108.300	107.195
Relative error η_j in %	0.19	0.01	0.04	0.28	0.18

Table 13. Example 3 – Results of the fault diagnosis of channel lengths in NMOS transistors M6, M7, M8, M9, M10 (computational time 201 s).

Symbols of the NMOS transistors	M6	M7	M8	M9	M10
The nominal value of L in nm	100.000	100.000	100.000	100.000	100.000
The actual value of L in nm	113.000	103.000	106.000	113.000	111.000
The values provided by the method in nm	113.176	103.156	106.042	113.779	111.014
Relative error η_j in %	0.16	0.15	0.04	0.69	0.01

Table 14. Example 3 – Results of the fault diagnosis of channel lengths in NMOS transistors M6, M7, M8, M9, M10 (computational time 628 s).

Symbols of the NMOS transistors	M6	M7	M8	M9	M10
The nominal value of L in nm	100.000	100.000	100.000	100.000	100.000
The actual value of L in nm	106.500	165.000	135.000	145.000	107.000
The values provided by the method in nm	106.718	164.966	134.806	144.812	106.920
Relative error η_j in %	0.20	0.02	0.14	0.13	0.07

7. Conclusion

The verification method presented in this paper enables to efficiently diagnose multiple soft faults in middle-sized linear circuits. It is general and is not limited only to double or triple faults with small parameter deviations. The proposed approach is based on the Powell's minimization method without gradients. In consequence, no sensitivity analysis of a circuit under test is required, what considerably simplifies its implementation and improves the diagnostic process. The method employs the measured output voltage at several frequencies, but the measurements are simple and use standard instrumentation. The minimization procedure based on the Powell's method is fast and does not require great computing power. It is easy to implement and reliable. In all considered cases, where the set of the tested elements did not contain a subset of elements creating an ambiguity group, the proposed method gave correct results. The sets of parameters which are unambiguously diagnosed can be selected on the basis of the testability analysis. The method fails if the deviations of the diagnosed parameters do not influence noticeably the tested voltages, measured with an assumed accuracy. Although the method is dedicated to linear circuits, it can be adapted to multiple soft fault diagnosis of nonlinear ones including CMOS circuits designed in a sub-micrometre technology. In this case the computational complexity of the minimization procedure, implemented in DELPHI, is similar to the complexity of the procedure used in linear circuits. However, the circuit analyses required by the diagnostic method are more complex because the MOS transistor model BSIM 4.6 is very intricate. These analyses are carried out using IsSPICE 4 and the communication between the DELPHI and IsSPICE environments is very time-consuming. Thus, the method enables to diagnose small- and middle-sized CMOS circuits designed in a sub-micrometre technology, but it is more difficult to implement and less efficient.

Acknowledgement

This work was supported in part by Polish Ministry of Science and Higher Education under Grant DIR/WK/2016/03 and in part by the Statutory Activities of Lodz University of Technology 5418DzS.

References

[1] Aminian, M., Aminian, F. (2007). A modular fault-diagnosis system for analog electronic circuits using neural networks with wavelet transform as a preprocessor. *IEEE Trans. Instrum. Meas.*, 56, 1546–1554.

[2] Bilski, P., Wojciechowski, J.M. (2011). Rough-sets-based reduction for analog systems diagnostics. *IEEE Trans. Instrum. Meas.*, 60, 880–890.

[3] Bhunia, S., Raychowdhury, A., Roy, K. (2005). Defect oriented testing of analog circuits using wavelet analysis of dynamic supply current. *J. Electron Test.*, 21, 147–159.

[4] Catelani, M., Fort, A. (2002). Soft fault detection and isolation in analog circuits: some results and a comparison between a fuzzy approach and radial basis function networks. *IEEE Trans. Instrum. Meas.*, 51, 196–202.

[5] Czaja, Z., Zielonko, R. (2004). On fault diagnosis of analogue electronic circuits based on transformations in multi-dimensional spaces. *Measurement*, 35, 293–301.

[6] Czaja, Z. (2008). Using a square-wave signal for fault diagnosis of analog parts of mixed-signal electronic embedded systems. *IEEE Trans. Instrum. Meas.*, 57, 1589–1595.

[7] Dai, H., Souders, T.M. (1990). Time-domain testing strategies and fault diagnosis for analog systems. *IEEE Trans. Instrum. Meas.*, 19, 157–162.

[8] Deng, Y., Shi, Y., Zhang, W. (2012). An approach to locate parametric faults in nonlinear analog circuits. *IEEE Trans. Instrum. Meas*., 61, 358–367.

[9] Fedi, G., Manetti, S., Piccirilli, M.C., Starzyk, J. (1999). Determination of an optimum set of testable components in the fault diagnosis of analog linear circuits. *IEEE Trans. Circ. Syst.-I*, 46, 779–787.

[10] Gizopoulos, D. (2006). *Advances in electronic testing. Challenges and methodologies*. Springer, Dordrecht.

[11] Grasso, F., Luchetta, A., Manetti, S., Piccirilli, M.C. (2007). A method for the automatic selection of test frequencies in analog fault diagnosis. *IEEE Trans. Instrum. Measur*., 56, 2322–2329.

[12] Grzechca, D. (2011). Soft fault clustering in analog electronic circuits with the use of self organizing neural network. *Metrol. Meas. Syst.*, 18(4), 555–568.

[13] Grzechca, D. (2015). Construction of an expert system based on fuzzy logic for diagnosis of analog electronic circuits. *Int. J. Electron. Telecomm*., 61, 77–82.

[14] Han H., Wang H., Tian S., Zhang N. (2013). A new analog circuit fault diagnosis method based on improved Mahalanobis distance. *J. Electron Test.*, 29, 95–102.

[15] Hałgas, S., Tadeusiewicz, M. (2008). Multiple soft fault diagnosis of analogue electronic circuits. *Procceedings of the International Conference on Signals and Electronic Systems ICSES'2008*, Kraków, Poland, 533–536.

[16] Jahangiri, M., Razaghian, F. (2014). Fault detection in analogue circuits using hybrid evolutionary algorithm and neural network. *Analog Int. Cir. Sig. Proc*., 80, 551–556.

[17] Jantos, P., Grzechca, D., Rutkowski. J. (2012). Evolutionary algorithms for global parametric fault diagnosis in analogue integrated circuits. *Bull. Polish Acad. Scien*., 60, 133–142.

[18] Jiang Y., Wang Y., Luo H. (2015). Fault diagnosis of analog circuit based on a second map SVDD. *Analog Int. Cir. Sig. Proc*., 85, 395–404.

[19] Kabisatpathy, P., Barua, A., Sinha, S. (2005). *Fault diagnosis of analog integrated circuits*. Springer, Dordrecht.

[20] Long, B., Li, M., Wang, H., Tian, S. (2013). Diagnostics of analog circuits based on LS_SVM using time-domain features. *Circuits Syst. Signal Process*., 32, 2683–2706.

[21] Materka, A., Strzelecki, M. (1996). Parametric testing of mixed-signal circuits by ANN processing of transient responses. *J. Electron Test.*, 9, 187–202.

[22] Papakostas, D.K., Hatzopoulos, A.A. (2008). A unified procedure for fault detection of analog and mixed-mode circuits using magnitude and phase components of the power supply current spectrum. *IEEE Trans. Instrum. Measur*., 57, 2589–2995.

[23] Papakostas D.K., Hatzopoulos A.A. (2010). Improved analogue fault coverage estimation using probability analysis. *Int. J. Circ. Theory Appl*., 38, 503–514.

[24] Robotycki, A., Zielonko, R. (2002). Fault diagnosis of analog piecewise linear circuits based on homotopy. *IEEE Trans. Instrum. Meas.*, 51, 867–881.

[25] Sałat, R., Osowski, S. (2011). Support Vector Machine for soft fault location in electrical circuits. *J. Intelligent Fuzzy Systems*., 22, 21–31.

[26] Sindia, S., Agrawal, V.D,. Singh, V. (2012). Parametric fault testing of non-linear analog circuits based on polynomial and V-transform coefficients. *J. Electron Test*., 28, 757–771.

[27] Tadeusiewicz, M., Korzybski, M. (2000). A method for fault diagnosis in linear electronic circuits. *Int. J. Circ. Theory Appl*., 28, 245–262.

[28] Tadeusiewicz, M., Hałgas, S., Korzybski, M. (2002). An algorithm for soft-fault diagnosis of linear and nonlinear circuits. *IEEE Trans. Circ. Syst.-I*, 49, 1648–1653.

[29] Tadeusiewicz, M., Hałgas, S. (2006). An algorithm for multiple fault diagnosis in analogue circuits. *Int. J. Circ. Theory Appl.*, 34, 607–615.

[30] Tadeusiewicz, M., Hałgas, S. (2015). A new approach to multiple soft fault diagnosis of analog BJT and CMOS circuits. *IEEE Trans. Instrum. Measur.*, 64, 2688–2695.

[31] Tadeusiewicz, M., Kuczyński, A., Hałgas, S. (2015). Catastrophic fault diagnosis of a certain class of nonlinear analog circuits. *Circuits Syst. Signal Process.*, 34, 353–375.

[32] Tadeusiewicz, M., Hałgas, S. (2016). Multiple soft fault diagnosis of DC analog CMOS circuits designed in nanometer technology, *Analog Int. Cir. Sig. Proc.*, 88, 65–77.

[33] Tadeusiewicz, M., Hałgas, S. (2016). Diagnosis of soft spot short defects in analog circuits considering the thermal behaviour of the chip. *Metrol. Meas. Syst.*, 23(2), 239–250.

[34] Xie, Y., Li, X., Xie, S., Xie, X., Zhou, Q. (2014). Soft fault diagnosis of analog circuits via frequency response function measurements. *J. Electron Test.*, 30, 243–249.

[35] Yang, C., Tian, S., Long, B., Chen, F. (2011). Methods of handling the tolerance and test-point selection problem for analog-circuit fault diagnosis. *IEEE Trans. Instrum. Meas.*, 60, 176–185.

[36] Yu, W., He, Y. (2015). Analog circuit fault diagnosis via sensitivity computation. *J. Electron Test.*, 31, 119–122.

[37] Yuan, L., He, Y., Huang, J., Sun, Y. (2010). A new neural-network-based fault diagnosis approach for analog circuits by using kurtosis and entropy as a preprocessor. *IEEE Trans. Instrum. Meas.*, 59, 586–595.

[38] Zhou, Q.Z., Xie, Y.L., Li, X.F., Bi, D.J., Xie, X., Xie, S.S. (2014). Methodology and equipments for analog circuit parametric faults diagnosis based on matrix eigenvalues. *IEEE Trans. Appl. Superconductivity*, 24, 1–6.

[39] Mathews, J.H., Fink, K.K. (2004). *Numerical methods using MATLAB*. Prentice-Hall.

[40] Press, W.H., Teukolsky, S.A., Vetterling, W.T., Flannery, B.P. (1992). *Numerical Recipes in C (2nd Ed.), The Art of Scientific Computing*. Cambridge University Press.

[41] *IsSPICE4 User's Guides, vol. 1,2, rev 04/08*. (Intusoft, 2008).

[42] Baker, R. *CMOS Circuit Design, Layout and Simulation*. (Wiley-IEEE Pres, 2010).

Appendix

A sketch of the Fibonacci method

The Fibonacci method is a procedure for finding the minimum of a variable function $\hat{f}(\lambda)$ within the range (λ^-, λ^+) by narrowing this range in a systematic way. The method is described in detail in the reference [39]. The main idea of this method is as follows.

The method minimizes the function $\hat{f}(\lambda)$ over the range (λ^-, λ^+), where $\hat{f}(\lambda)$ is unimodal. Let L^0 be a length of the range (λ^-, λ^+). To find $\lambda = \widetilde{\lambda}$ that minimizes the function the internal points λ_1 and λ_2 are selected so that $\lambda_1 = \lambda^- + \left(L^0 - \frac{L^0}{\rho}\right)$, $\lambda_2 = \lambda^- + \frac{L^0}{\rho}$ (see Fig. A.1), where $\rho \cong 1.618$ [39]. If $\hat{f}(\lambda_1) > \hat{f}(\lambda_2)$, as in Fig. A.1, $\widetilde{\lambda}$ must lie in the range (λ_1, λ^+) whose length is labelled L^1. Otherwise, it must lie between λ^-, λ_2, creating the range (λ^-, λ_2). For an appropriate range the internal points λ_3 and λ_4 are selected similarly to λ_1 and λ_2 in the range (λ^-, λ^+). The procedure is repeated leading to a sequence of intervals L^0, L^1, L^2, …, so that $\dfrac{L^j}{L^{j+1}} = \rho = 1.618$ and each of the intervals includes $\widetilde{\lambda}$. Thus, after k steps the obtained interval $L^k = L^0\rho^{-k}$ and $\widetilde{\lambda} \in L^k$. The procedure is terminated once the length of L^k is less than the required accuracy of $\widetilde{\lambda}$.

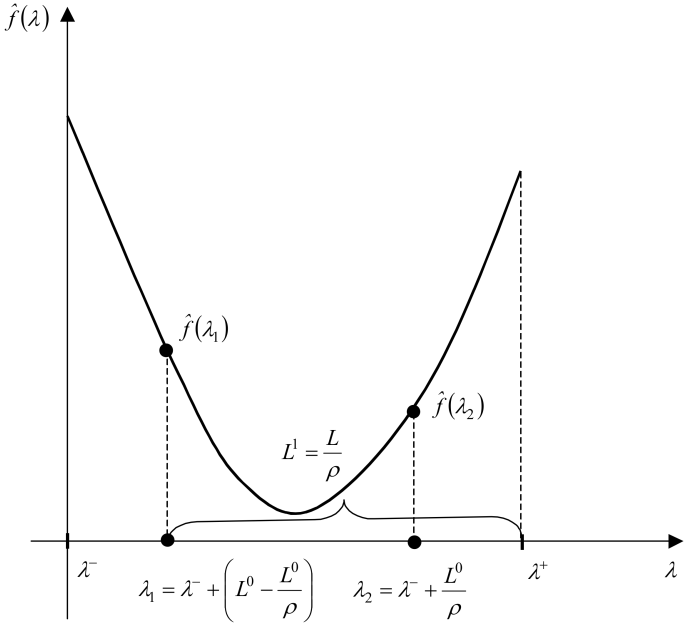

Fig. A.1. Illustration of the Fibonacci method.